5,6-Dihydro-5,6-Epoxymultiplolide A, Cytosporone C and Uridine Production by Diaporthe hongkongensis an Endophytic Fungus from Minquartia guianensis

Andrei da Silva Alexandre , David Ribeiro da Silva , Luana Lopes Casas , Cecilia Veronica Nunez *

Posted Date: 14 February 2025

doi: 10.20944/preprints202502.1097.v1

Keywords: fungus; parboiled rice; secondary metabolites; NMR spectroscopy; multiplolide; polyketide; nucleoside

 doi:10.20944/preprints202502.1097.v1

Article

5,6-Dihydro-5,6-epoxymultiplolide A, Cytosporone C and Uridine Production by *Diaporthe hongkongensis* an Endophytic Fungus from *Minquartia guianensis*

Andrei da Silva Alexandre [1,2], Luana Lopes Casas [1,2], David Ribeiro da Silva [1] and Cecilia Veronica Nunez [1,2,*]

[1] Bioprospection and Biotechnology Laboratory; Technology and Innovation Coordination; National Institute of Amazonian Research, 69067-375, Manaus – AM, Brazil

[2] Graduate Program in Biotechnology and Natural Resources of the Amazon, School of Health Sciences, Amazonas State University, 69050-010, Manaus – AM, Brazil

* Correspondence: cecilia@inpa.gov.br (C.V.N.)

Abstract: Endophytic fungi are valuable sources of bioactive secondary metabolites, with potential applications in pharmaceutical and agricultural fields. This study explores the metabolic potential of *Diaporthe hongkongensis*, an endophytic fungus isolated from *Minquartia guianensis*. The fungus was cultivated on parboiled rice under static and dark conditions for 28 days, leading to the isolation of three compounds: 5,6-dihydro-5,6-epoxymultiplolide A (**1**), cytosporone C (**2**), and uridine (**3**). Structural identification was carried out using nuclear magnetic resonance (NMR) spectroscopy and mass spectrometry. The results revealed the metabolic versatility of *D. hongkongensis*, as demonstrated by its ability to produce structurally diverse secondary metabolites with biological relevance. The identification of a known antifungal compound and a lactone derivative underscores the biosynthetic potential of this endophytic fungus, while the isolation of a nucleoside expands the chemical repertoire of fungal metabolites, suggesting possible roles in cellular metabolism and stress adaptation. These findings reinforce the role of endophytic fungi as prolific sources of structurally diverse and potentially bioactive natural products, supporting further exploration of their biotechnological applications.

Keywords: fungus; parboiled rice; secondary metabolites; NMR spectroscopy; multiplolide; polyketide; nucleoside

1. Introduction

Fungi of the genus *Diaporthe* are globally distributed and exhibit diverse lifestyles, including roles as endophytes, pathogens, and saprobes. Notably, they are prolific producers of secondary metabolites, such as polyketides, terpenoids, and alkaloids, which possess a wide range of biological activities, including cytotoxic, antifungal, antibacterial, antiviral, antioxidant, anti-inflammatory, and phytotoxic effects [1–4]. Despite these findings, the potential of *Diaporthe hongkongensis*, a relatively underexplored species, remains largely untapped.

The Amazon rainforest offers a vast reservoir of biological and chemical diversity. This region harbors countless plant species, many of which maintain complex relationships with endophytic fungi. These symbiotic fungi are considered a sustainable and underutilized resource for bioprospecting [5]. Among Amazonian flora, *Minquartia guianensis* Aubl. (family Coulaceae) is an ecologically and culturally significant tree species. Its dense wood has applications in construction, and it has traditional uses in medicine among local communities [6,7]. Despite its ecological and economic importance, the microbial endophytes associated with *M. guianensis* have been minimally studied, leaving a significant gap in understanding their chemical and ecological roles.

 doi:10.20944/preprints202502.1097.v1

The chemical investigation of endophytic fungi such as *D. hongkongensis* is particularly significant due to their potential to yield novel bioactive compounds. For example, recent studies on *Diaporthe* species have identified metabolites with promising antibacterial, antifungal, and anticancer activities [8–10]. By linking the fungal biodiversity of the Amazon to its chemical potential, this research contributes to the growing field of natural product discovery and highlights the untapped potential of microbial symbionts in biodiverse ecosystems.

In this context, the objectives of this study were to isolate and identify *D. hongkongensis* from *M. guianensis*, characterize its secondary metabolites, and explore its potential as a source of bioactive compounds. This research underscores the importance of preserving Amazonian biodiversity and integrating fungal bioprospecting into strategies for sustainable development.

2. Materials and Methods

2.1. Fungal Material

The endophytic strain *D. hongkongensis* was isolated from fresh, healthy leaves of *Minquartia guianensis* collected in May 2014, in the Reserva Florestal Adolpho Ducke, Manaus, Amazonas, Brazil, at coordinates: 2º55'24.69" S 59º58'26.12" W. The study was registered in the National System for the Management of Genetic Heritage and Associated Traditional Knowledge (SisGen/MMA – BR) under number: ACCD2F4.

The fungus was isolated under sterile conditions from the inner tissue of the leaves, following a previously described isolation protocol [11]. Identification was carried out using molecular biological techniques involving DNA amplification and sequencing of the ITS region. The results showed that the fungus was closely related to *D. hongkongensis*, with a 99% similarity in the ITS sequence. Combined with morphological characteristics, the strain was identified as *D. hongkongensis*. The fungal strain was deposited in the culture collection of the Laboratory of Bioprospecting and Biotechnology at the National Institute of Amazonian Research (INPA).

2.2. Fermentation, Extraction, and Isolation of Compounds

The strain was cultured on potato dextrose agar (PDA) at 28 °C for five days. The agar, containing the fungal growth, was then excised, and aseptically inoculated into three 500 mL Erlenmeyer flasks, each containing a parboiled rice medium. The rice medium consisted of 50 g of rice and 100 mL of distilled water, sterilized at 120 °C for 15 minutes prior to use. The flasks were incubated for 28 days at 25 °C under static and light-free conditions. After the incubation period, the rice culture was extracted four times with ethyl acetate (EtOAc) using an ultrasonic bath (Unique, Ultra Cleaner, Brazil) for 20 minutes. Additionally, an uninoculated rice medium was incubated and extracted in the same manner after 28 days, serving as a negative control. The resulting extracts were filtered and concentrated using a rotary evaporator at 40 °C [12,13]. The EtOAc extract (5.0 g) was subjected to chromatographic separation on a Sephadex LH-20 column eluted with methanol (MeOH). A total of 23 fractions were obtained and subsequently grouped based on separation patterns observed on silica TLC analytical plates (Sigma-Aldrich). Fraction DhC2.1F7-8 was further separated on a silica gel 60 (SiO_2, 230-400 mesh) column chromatography eluted with dichloromethane and EtOAc mixtures, yielding compound **1** (2.0 mg). Similarly, fraction DhC2.6F11-15 was processed on a SiO_2 column eluted with dichloromethane and EtOAc mixtures, affording compound **2** (4.0 mg). Finally, fraction DhC2.5.1F3-5 was isolated using a column over SiO_2, eluted with dichloromethane and MeOH mixtures, to yield compound **3** (1.5 mg).

2.3. Structural Identification

The substances were solubilized in deuterated acetone (Cambridge Isotope Laboratories) and deuterated dimethyl sulfoxide (DMSO-d_6, Cambridge Isotope Laboratories). The nuclear magnetic resonance (NMR) spectra were obtained using a Fourier 300 (Bruker) spectrometer at the Analytical

 doi:10.20944/preprints202502.1097.v1

Center of the INPA, operating at 300 MHz for ^{1}H uni and bidimensional analyses, such as COSY (Correlated Spectroscopy) and HSQC (Heteronuclear Single Quantum Correlation), and at 75 MHz for ^{13}C (BroadBand Decoupling [BBD]) and Distortionless Enhancement by Polarization Transfer [DEPT] 135°). Chemical shifts (δ) were expressed in parts per million and coupling constants (*J*) were expressed in Hz to describe peak multiplicities, using tetramethylsilane (TMS) as an internal standard.

Mass spectrometry analyses were performed in both positive and negative ionization modes using an ESI (Electrospray Ionization) source. LC-DAD-MS analyses (Ultra-Fast Liquid Chromatography coupled to a Diode Array Detector and Mass Spectrometer) were conducted using a Prominence UFLC chromatograph (Shimadzu), equipped with an LC-20AT binary pump, SPD-M20A diode array detector, SIL-20A automatic injector, and a MicroTOF-Q II mass spectrometer (Bruker).

3. Results

The mycelia and culture medium of the endophytic fungus *D. hongkongensis* were extracted with EtOAc. This extract was concentrated and then repeatedly chromatographed over Sephadex LH-20 and SiO_2 to yield three compounds, a macrolide 5,6-dihydro-5,6-epoxymultiplolide A (**1**), together with the known cytosporone C (**2**) and uridine (**3**) (Figure 1).

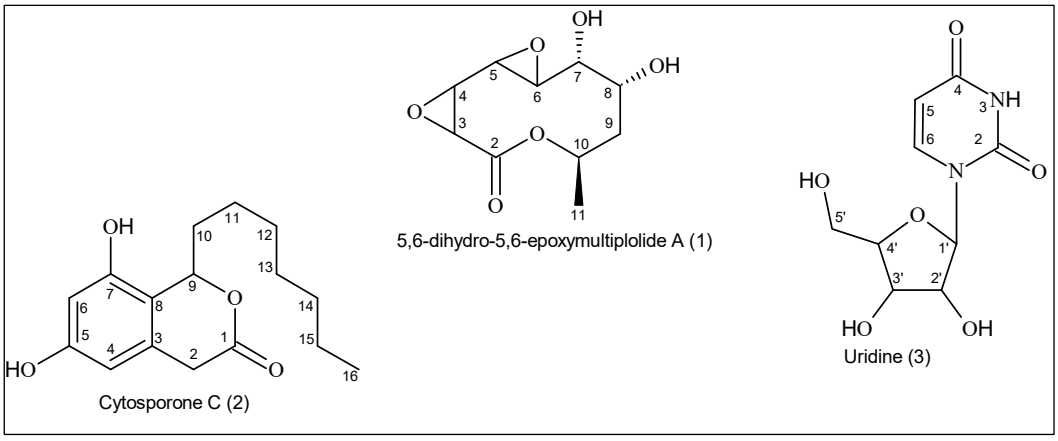

Figure 1. Chemical structure of the substances isolated from the ethyl acetate extract of the fungus *D. hongkongensis*.

3.1. Structural Identification of the Compounds

3.1.1. 5,6-Dihydro-5,6-epoxymultiplolide A (1)

Compound **1** was isolated as a colorless oil. Its molecular formula, $C_{10}H_{14}O_6$, was determined by high-resolution electrospray ionization time-of-flight mass spectrometry (HR-ESI-TOF-MS), which displayed a molecular ion peak at *m/z* 253.0683 $[M + Na]^+$.

The ^{1}H NMR spectrum (300 MHz, acetone-d_6) displayed key signals characteristic of the compound's structure. The epoxide ring was confirmed by the appearance of two doublets at δ 3.62 and δ 3.64 (J = 4.9 Hz), corresponding to geminal hydrogens at C-3 and C-4. A multiplet at δ 3.30 and a double doublet at δ 3.43 (J = 2.2, 0.6 Hz) were assigned to the oxygenated methine hydrogens H-5 and H-6, respectively. Other signals included δ 4.07 (multiplet) and δ 4.12 (ddd, J = 8.2, 2.2, 0.9 Hz) for the oxygenated hydrogens H-7 and H-8, as well as δ 1.49 (dd, J = 15.5, 5.0 Hz) and δ 2.29 (ddd, J = 15.5, 8.2, 3.6 Hz) for the H-9 methylene group. The alkene hydrogen was observed at δ 5.38 (ddq, J = 8.7, 6.6, 3.0, 1.3, H-10), and the methyl group at C-11 appeared as a doublet at δ 1.30 (J = 6.62 Hz).

The ^{13}C NMR spectrum (75 MHz, acetone-d_6) revealed ten carbon signals consistent with the molecular formula. The lactone carbonyl group was identified at δ 166.6 (C-2). Other significant

 doi:10.20944/preprints202502.1097.v1

signals included oxygenated sp^3 carbons at δ 51.2 (C-3), δ 52.8 (C-4), δ 55.9 (C-5), δ 50.3 (C-6), δ 69.8 (C-7), δ 66.9 (C-8), and δ 68.0 (C-10). The methylene carbon (C-9) resonated at δ 35.3, while the methyl carbon (C-11) was observed at δ 17.7.

The HSQC spectrum confirmed direct hydrogen-carbon one-bond correlations, facilitating assignments of hydrogens to their corresponding carbons. The epoxide hydrogens at δ 3.62 and δ 3.64 were correlated with δ 51.2 (C-3) and δ 52.8 (C-4), respectively. The oxygenated methine hydrogens δ 3.30 (H-5) and δ 3.43 (H-6) showed correlations with δ 55.9 (C-5) and δ 50.3 (C-6). Similarly, the hydrogen at δ 4.07 (H-7) was correlated with δ 69.8 (C-7), and the methyl hydrogens at δ 1.30 (H-11) were linked to δ 17.7 (C-11).

The HMBC spectrum provided critical long-range correlations, confirming the connectivity of the molecule. The epoxide hydrogens (H-3 and H-4) at δ 3.62 and δ 3.64 showed correlations with the lactone carbonyl carbon (C-2, δ 166.6). H-5 (δ 3.30) exhibited correlations with C-3, C-4 and C-7 (δ 51.2, 52.8 and 69.8), while H-6 (δ 3.43) showed correlations with C-4 (δ 52.8) and C-5 (δ 55.9). The methyl hydrogens (H-11, δ 1.30) displayed correlations with the oxygenated methine carbon (C-10, δ 68.0) and methylene carbon δ 35.3 (C-9).

The COSY spectrum further supported the structure by showing H-H coupling relationships. The epoxide hydrogens (H-3 and H-4) were coupled to each other, confirming their proximity. H-6 (δ 3.43) was coupled to H-8 (δ 4.12), while H-8 was coupled to the methylene hydrogens H-9 (δ 1.49 and δ 2.29). Additionally, sequential couplings were observed between H-10 and H-11 (δ 1.30).

The data were compared with the literature confirming the chemical structure [14].

3.1.2. Cytosporone C (2)

Compound **2** was isolated as a yellow amorphous solid. The molecular formula was determined to be $C_{16}H_{22}O_4$ based on HR-ESI-TOF-MS, which showed a $[M + H]^+$ peak at m/z 279.1591 (calculated for $C_{16}H_{23}O_4$, m/z 279.1605).

The ^1H NMR spectrum (300 MHz, acetone-d_6) revealed characteristic signals for the aromatic hydrogens at δ 6.34 (H-6) and δ 6.24 (H-4), as well as a deshielded methine hydrogen at δ 5.54 (H-9), indicative of its proximity to oxygenated carbons. Methylene groups were observed at δ 3.79 and 3.43 (H-2) and in the aliphatic region at δ 1.86–1.27. A terminal methyl group resonated as a triplet at δ 0.87 (H-16, J = 6.9 Hz).

The ^{13}C NMR spectrum (75 MHz, acetone-d_6) supported these observations, with signals consistent with two aromatic carbons (δ 158.1, C-5; δ 153.7, C-7), a ketone carbonyl (δ 170.1, C-1), and an oxygenated methine carbon (δ 77.6, C-9), along with aliphatic and methyl carbons.

The HSQC experiment revealed direct one-bond correlations between hydrogens and their attached carbons, facilitating the assignment of δ 6.34 (H-6) to δ 101.0 (C-6), δ 6.24 (H-4) to δ 105.3 (C-4), and δ 5.54 (H-9) to δ 77.6 (C-9). The methylene hydrogens at δ 3.79 and 3.43 (H-2) were correlated to δ 34.5 (C-2), while the terminal methyl hydrogens at δ 0.87 (H-16) were linked to δ 13.4 (C-16).

Long-range correlations from the HMBC spectrum provided key insights into the molecular connectivity. The aromatic hydrogen at δ 6.34 (H-6) showed correlations with δ 105.3 (C-4), δ 112.9 (C-8), δ 153.7 (C-7), and δ 158.1 (C-5), while δ 6.24 (H-6) correlated with δ 158.1 (C-5), δ 112.9 (C-8), δ 101.0 (C-6), and δ 34.5 (C-2). The methine hydrogen at δ 5.54 (H-9) exhibited correlations with δ 112.9 (C-8), δ 153.7 (C-7), δ 132.3 (C-3), δ 170.1 (C-1), confirming its position adjacent to an oxygenated carbon and an aromatic ring. The methylene hydrogens at δ 3.79 and 3.43 (H-2) were correlated with the carbonyl carbon at δ 170.1 (C-1) and the aromatic carbon at δ 132.3 (C-3).

The COSY spectrum established spin-spin couplings between adjacent hydrogens. The methine hydrogen at δ 5.54 (H-9) was coupled to the methylene hydrogen at δ 1.80 (H-10) which were in turn coupled to δ 1.45. Sequential couplings were observed from H-11 through H-15 (δ 1.27–1.40), terminating with the terminal methyl group (H-16, δ 0.87).

The data were compared with the literature confirming the chemical structure [15].

3.1.3. Uridine (3)

 doi:10.20944/preprints202502.1097.v1

Compound **3** was obtained as a white solid. HR-ESI-TOF-MS revealed a $[M + H]^+$ peak at *m/z* 244.0766 (calculated for $C_9H_{13}N_2O_6$, *m/z* 245.0768), corresponding to a molecular formula of $C_9H_{12}N_2O_6$.

The structural identification of **3** was carried out based on one-dimensional and two-dimensional NMR spectroscopy data. In the ^1H NMR spectrum (300 MHz, DMSO-d_6) NH hydrogen of the uracil base appeared as a singlet at δ 11.31, which is characteristic of an amidic hydrogen in a pyrimidine system. The H-6 hydrogen was observed at δ 7.87 (d, *J* = 8.0 Hz), showing a characteristic coupling with H-5 at δ 5.63 (d, *J* = 8.0 Hz). This coupling pattern confirmed the expected spin system of the uracil moiety. The H-1' anomeric hydrogen of the ribose appeared as a doublet at δ 5.76 (d, *J* = 5.4 Hz), which is indicative of a β-glycosidic bond between the ribose and the uracil base. Hydroxyl hydrogens at δ 5.42 (2'-OH), δ 5.16 (3'-OH), and δ 5.16 (5'-OH) suggested the presence of free hydroxyl groups on the ribose ring, confirming the unmodified nature of the sugar moiety. Multiple peaks between δ 4.01 and 3.58 corresponded to the ribose ring hydrogens, including those at C-2', C-3', C-4', and C-5'. These chemical shifts and coupling patterns are consistent with the expected values for a ribofuranose ring in uridine.

The ^{13}C NMR spectrum (75 MHz, DMSO-d_6) revealed the presence of ten distinct carbon resonances, corresponding to the uracil and ribose units. The uracil ring carbons were observed at δ 151.1 (C-2) and δ 163.6 (C-4), which are associated with the carbonyl groups of the pyrimidine system. Additionally, the signals at δ 102.2 (C-5) and δ 141.1 (C-6) were consistent with values for the conjugated uracil ring. The ribose sugar was identified by the anomeric carbon (C-1') at δ 88.1. The remaining ribose carbons were found at δ 74.0 (C-2'), δ 70.3 (C-3'), δ 85.2 (C-4'), and δ 61.3 (C-5'), further confirming the ribofuranose configuration. The downfield chemical shifts of C-2', C-3', and C-5' indicated the presence of hydroxyl groups at these positions, supporting the unmodified nature of the ribose unit.

The HSQC spectrum allowed the assignment of carbon- hydrogen pairs. The correlation between δ 5.76 (H-1') and δ 88.1 (C-1') reinforced the identity of the anomeric center, while the connections between C-2' (δ 74.0) and its respective hydrogen further established the ribose framework.

The HMBC spectrum provided crucial long-range correlations, particularly confirming glycosidic connectivity and the electronic environment of the uracil base. The correlation between H-1' (δ 5.76) and C-2 (δ 151.1) and C-6 (δ 141.1) confirmed the direct attachment of the ribose to the uracil base. Additionally, the correlation between H-5 (δ 5.63) and C-4 (δ 163.6) and C-6 (δ 141.1) further supported the structure of the pyrimidine system. The hydroxyl hydrogens (2'-OH, 3'-OH, and 5'-OH) exhibited interactions with their respective ribose carbons, reinforcing the integrity of the sugar moiety.

Finally, the COSY experiment revealed coupling interactions, confirming the connectivity between the sugar hydrogens. The H-1' (δ 5.76) coupled with H-2' (multiplet at δ 4.01–3.95), establishes the glycosidic bond. Additional coupling between H-2', H-3', H-4', and H-5' confirmed the expected sequential connectivity of the ribose ring, further supporting the assigned structure.

The data were compared with the literature confirming the chemical structure [16].

3.1.4. NMR Measurements

5,6-dihydro-5,6-epoxymultiplolide A (**1**). ^1H NMR (300 MHz, acetone-d_6): δ 3.62 (d, *J* = 4.9 Hz, H-3), 3.64 (d, *J* = 4.9 Hz, H-4), 3.30 (m, H-5), 3.43 (dd, *J* = 2.2, 0.6 Hz, H-6), 4.07 (m, H-7), 4.12 (ddd, *J* = 8.2, 2.2, 0.9 Hz, H-8), 1.49 (dd, *J* = 15.5, 5.0 Hz, H-9), 2.29 (ddd, *J* = 15.5, 8.2, 3.6 Hz, H-9), 5.38 (ddq, *J* = 8.7, 6.6, 3.0, 1.3, H-10), 1.30 (d, *J* = 6.62 Hz, H-11). ^{13}C NMR (75 MHz, acetone-d_6): δ 166.6 (C-2), 51.2 (C-3), 52.8 (C-4), 55.9 (C-5), 50.3 (C-6), 69.8 (C-7), 66.9 (C-8), 35.3 (C-9), 68.0 (C-10), 17.7 (C-11). Molecular formula: $C_{10}H_{14}O_6$ by HR-ESI-TOF-MS (*m/z* 253.0682 $[M + Na]^+$).

Cytosporone C (**2**). ^1H NMR (300 MHz, acetone-d_6): δ 6.34 (1H, d, *J* = 0.6 Hz, H-6), 6.24 (1H, d, *J* = 0.6 Hz, H-4), 5.54 (1H, dd, *J* = 8.8, 5.0 Hz, H-9), 3.79 (1H, d, *J* = 19.2 Hz, H-2), 3.43 (1H, d, *J* = 19.2 Hz, H-2), 1.86 (1H, m, H-10), 1.80 (1H, m, H-10), 1.55 (1H, m, H-11), 1.45 (1H, m, H-11), 1.27–1.40 (8H, m,

 doi:10.20944/preprints202502.1097.v1

H12–15), 0.87 (3H, t, *J* = 6.9 Hz, H-16). ^{13}C NMR (75 MHz, acetone-d_6): δ 170.1 (C-1), 158.1 (C-5), 153.7 (C-7), 132.3 (C-3), 112.9 (C-8), 105.3 (C-4), 101.0 (C-6), 77.6 (C-9), 35.6 (C-10), 34.5 (C-2), 31.7 (C-14), 29.0 (C- 13), 29.0 (C-12), 25.5 (C-11), 22.4 (C-15), 13.4 (C-16). Molecular formula: $C_{16}H_{22}O_4$ by HR-ESI-TOF-MS (*m*/*z* 279.1591 [M + H] $^+$).

Uridine (**3**). ^{1}H NMR (300 MHz, DMSO-d_6): δ 11.31 (1H, H-3), 7.87 (1H, d, *J* = 8.0 Hz, H-6), 5.76 (1H, d, *J* = 5.4 Hz, H-1′), 5.63 (1H, d, *J* = 8.0 Hz, H-5), 5.42 (1H, 2′-OH), 5.16 (1H, 3′-OH), 5.16 (1H, 5′-OH), 4.01 (1H, m, H-2′), 3.95 (1H, m), 3.83 (1H, m, H-4′), 3.58 (2H, t, *J* = 11 Hz, H-5′). ^{13}C NMR (75 MHz, DMSO-d_6): δ 151.1 (C-2), 163.6 (C-4), 102.2 (C-5), 141.1 (C-6), 88.1 (C-1'), 74.0 (C-2'), 70.3 (C-3'), 85.2 (C-4'), 61.3 (C-5'). Molecular formula: $C_9H_{12}N_2O_6$ by HR-ESI-TOF-MS (*m*/*z* 244.0766 [M + H] $^+$).

4. Discussion

The isolation of 5,6-dihydro-5,6-epoxymultiplolide A (**1**), cytosporone C (**2**) and uridine (**3**) from the endophytic fungus *D. hongkongensis* underscores the importance of optimizing cultivation conditions to stimulate secondary metabolite production. *D. hongkongensis* was cultured on parboiled rice under static conditions at 25 °C in the dark for 28 days. This methodological approach was crucial for inducing the production of secondary metabolites, suggesting that nutrient availability, environmental stress, and cultivation parameters play an integral role in the biosynthetic activity of endophytes [12,17]. The use of parboiled rice as a cultivation medium is particularly noteworthy. Parboiled rice is a carbon- and nitrogen-rich substrate that supports fungal growth while providing a complex matrix that mimics the nutrient heterogeneity of the natural host environment. This substrate has been used in natural products research to induce secondary metabolite production, as it creates a semisolid matrix with low water activity, a condition known to upregulate secondary metabolism in fungi [12,18,19]. The static cultivation mode, combined with prolonged incubation in the dark, likely mimics the low-oxygen and light-deprived environments fungi experience in their natural endophytic niche, further triggering the expression of biosynthetic gene clusters responsible for metabolite production [17].

The isolation of 5,6-dihydro-5,6-epoxymultiplolide A (**1**) represents a significant addition to the multiploidy family of metabolites. Although less commonly reported, this compound—previously isolated from *Phomopsis* sp. (the asexual state of *Diaporthe*)—is characterized by the presence of an epoxide group and a lactone moiety. These structural features are often associated with bioactivity, including cytotoxic, antifungal, and antihyperlipidemic properties [14,20,21]. The epoxide group, in particular, is known to contribute to the reactivity and bioactivity of natural products, making this compound a promising candidate for further biological evaluation [22]. Moreover, the biosynthesis of macrolides is believed to involve complex polyketide synthase (PKS) pathways, which are tightly regulated by environmental and genetic factors [23,24]. The production of this compound under the described cultivation conditions highlights the critical role of environmental cues in activating these biosynthetic pathways, suggesting that specific cultural parameters may influence metabolite yield and structural diversity.

Cytosporone C (**2**) is a polyketide previously reported in other *Diaporthe* species, and its isolation in this study suggests a conserved biosynthetic pathway within the genus. Cytosporone C has been shown to exhibit antifungal activity [24]. Its production may provide an ecological advantage to *D. hongkongensis* as an endophyte, aiding in fungal competition or modulating the plant microbiome. Additionally, it highlights the metabolic potential of endophytic fungi as promising sources for biotechnological applications, including biocontrol and antifungal drug discovery.

Uridine (**3**) is a biologically significant nucleoside with diverse scientific and biotechnological applications. It plays a crucial role in metabolism, serving as a key precursor in nucleotide biosynthesis and influencing glucose and lipid homeostasis [26]. The regenerative effects of uridine in peripheral nerve injuries have been demonstrated in a rat model, highlighting its potential role in nerve repair and regeneration [27]. Its neuroprotective effects have been explored for cognitive enhancement and Alzheimer's disease treatment, particularly in formulations combining uridine,

 doi:10.20944/preprints202502.1097.v1

choline, and DHA [28]. Additionally, uridine derivatives contribute to antiviral, anticancer, and antibiotic drug development by targeting intracellular pathways [29].

From an ecological and functional perspective, the production of 5,6-dihydro-5,6-epoxymultiplolide A, cytosporone C and uridine by *D. hongkongensis* likely reflects adaptive biochemical strategies that enhance fungal survival and interaction within its host environment [30,31]. 5,6-dihydro-5,6-epoxymultiplolide A and Cytosporone C, as secondary metabolites, may function in microbial competition, chemical signaling, or modulating host responses [32,33], while uridine, a fundamental nucleoside, could play a role in RNA metabolism, stress adaptation, and cellular regulation [34,35]. The biosynthetic capacity of *D. hongkongensis* suggests a dynamic interplay between endophyte and host, potentially influenced by evolutionary pressures to produce structurally diverse bioactive compounds [36,37]. Given the pharmaceutical and biotechnological relevance of these metabolites, further studies on the biosynthetic pathways and regulatory mechanisms governing their production could provide valuable insights for natural product discovery and metabolic engineering applications [38,39].

5. Conclusions

This study underscores the metabolic versatility of *D. hongkongensis*, demonstrating its capacity to produce structurally diverse and biologically relevant secondary metabolites. The successful isolation of these compounds highlights the effectiveness of targeted cultivation strategies in optimizing fungal biosynthetic potential. Beyond their chemical diversity, the identified metabolites suggest ecological and physiological roles that warrant further investigation, particularly in microbial interactions and host adaptation. These findings reinforce the significance of endophytic fungi as promising sources of bioactive compounds, encouraging future research into their biosynthetic pathways, regulatory mechanisms, and potential applications in biotechnology, pharmaceuticals, and agriculture. Expanding our understanding of fungal metabolism may pave the way for discovering new therapeutic agents and sustainable biotechnological solutions.

Author Contributions: Conceptualization, A.S.A. and C.V.N.; methodology, A.S.A, L.L.C.; formal analysis, A.S.A. and D.R.S.; resources, C.V.N.; writing—original draft preparation, A.S.A.; writing—review and editing, C.V.N.; funding acquisition, C.V.N.. All authors have read and agreed to the published version of the manuscript.

Funding: This research was funded by the National Council for Scientific and Technological Development – Brazil (CNPq), Coordenação de Aperfeiçoamento de Pessoal de Nível Superior – Brazil (CAPES) and Fundação de Amparo à Pesquisa do Estado do Amazonas (FAPEAM).

Data Availability Statement: The data presented in this study is available on request from the corresponding author. The data are part of an ongoing study.

Acknowledgments: We thank technicians Magno Perea Muniz, Sabrina Kelly Reis de Morais and Zelina Torres from the Central Analítica do Laboratório Temático de Química de Produtos Naturais (CA-LTQPN) at INPA for their assistance with NMR and mass spectrometry analyses.

Conflicts of Interest: The authors declare no conflicts of interest.

References

1. Wei, W.; Khan, B.; Dai, Q.; Lin, J.; Kang, L.; Rajput, N.A.; Yan, W.; Liu, G. Potential of Secondary Metabolites of *Diaporthe* Species Associated with Terrestrial and Marine Origins. *J. Fungi (Basel)* **2023**, *9*(4), 453. doi: 10.3390/jof9040453
2. Noriler, S.A.; Savi, D.C.; Aluizio, R.; Palácio-Cortes, A.M.; Possiede, Y.M.; Glienke, C. Bioprospecting and Structure of Fungal Endophyte Communities Found in the Brazilian Biomes, Pantanal, and Cerrado. *Front. Microbiol.* **2018**, *9*, 1526. doi: 10.3389/fmicb.2018.01526

3. Matio-Kemkuignou, B.; Lambert, C.; Stadler, M.; Fogue, S.K.; Marin-Felix, Y. Unprecedented Antimicrobial and Cytotoxic Polyketides from Cultures of *Diaporthe africana* sp. nov. *J. Fungi (Basel)* **2023**, *9*(7), 781. doi: 10.3390/jof9070781
4. Manichart, N.; Laosinwattana, C.; Somala, N. et al. Physiological Mechanism of Action and Partial Separation of Herbicide–Active Compounds from the *Diaporthe* sp. Extract on *Amaranthus tricolor* L. *Sci. Rep.* **2023**, *13*, 18693. doi: 10.1038/s41598-023-46201-0
5. Araújo, K.S.; Alves, J.L.; Pereira, O.L.; de Queiroz, M.V. Five New Species of Endophytic *Penicillium* from Rubber Trees in the Brazilian Amazon. *Braz. J. Microbiol.* **2024**, *55*(4), 3051–3074. doi: 10.1007/s42770-024-01478-9
6. Camargo, J. L.; Ferraz, I. D. *Minquartia guianensis* Aubl. Manual de Sementes da Amazônia. INPA, p. 1–7, **2004**.
7. Costa-Lima, J.L.; Chagas, E.C.O. *Coulaceae* in Flora e Funga do Brasil. *Jardim Botânico do Rio de Janeiro*, **2020**. Available online: <https://floradobrasil.jbrj.gov.br/consulta/ficha.html?idDadosListaBrasil=618588>. Accessed on January 3, 2025
8. Majid, M.; Ganai, B.A.; Wani, A.H. Antifungal, Antioxidant Activity, and GC-MS Profiling of *Diaporthe amygdali* GWS39: A First Report Endophyte from *Geranium wallichianum*. *Curr. Microbiol.* **2024**, *82*(1), 40. doi: 10.1007/s00284-024-04023-x
9. Tanapichatsakul, C.; Monggoot, S.; Gentekaki, E.; Pripdeevech, P. Antibacterial and Antioxidant Metabolites of *Diaporthe* spp. Isolated from Flowers of *Melodorum fruticosum*. *Curr. Microbiol.* **2018**, *75*(4), 476–483. doi: 10.1007/s00284-017-1405-9
10. Yang, C.; Xing, S.; Wei, X.; Lu, J.; Zhao, G.; Ma, X.; Dai, Z.; Liang, X.; Huang, W.; Liu, Y.; Jiang, X.; Zhu, D. 12-O-Deacetyl-Phomoxanthone A Inhibits Ovarian Tumor Growth and Metastasis by Downregulating PDK4. *Biomed. Pharmacother.* **2024**, *175*, 116736. doi: 10.1016/j.biopha.2024.116736
11. Casas, L.L. *Bioprospecção de Fungos Endofíticos de Minquartia guianensis* Aubl. Dissertação de Mestrado, Universidade do Estado do Amazonas, **2016**, 86p.
12. Farinella, V.F.; Kawafune, E.S.; Tangerina, M.M.P.; Domingos, H.V.; Costa-Lotufo, L.V.; Ferreira, M.J.P. OSMAC Strategy Integrated with Molecular Networking for Accessing Griseofulvin Derivatives from Endophytic Fungi of *Moquiniastrum polymorphum* (Asteraceae). *Molecules* **2021**, *26*, 7316. doi: 10.3390/molecules26237316
13. Hidalgo, E.M.P. *Produtos Naturais de Bignonia magnifica W. Bull. (Bignoniaceae) e a Prospecção Metabólica dos Seus Fungos Endofíticos*. Tese de Doutorado, Universidade de São Paulo, **2023**, 170p.
14. Tan, Q.; Yan, X.; Lin, X.; Huang, Y.; Zheng, Z.; Song, S.; Lu, C.; Shen, Y. Chemical Constituents of the Endophytic Fungal *Phomopsis* sp. NXZ-05 of *Camptotheca acuminata*. *Helv. Chim. Acta* **2007**, *90*. doi: 10.1002/hlca.200790190
15. Brady, S.F.; Wagenaar, M.M.; Singh, M.P.; Janso, J.F.; Clardy, J. The Cytosporones, New Octaketide Antibiotics Isolated from an Endophytic Fungus. *Org. Lett.* **2000**, *2*(25). doi: 10.1021/ol006680s
16. Walczak, D.; Sikorski, A.; Grzywacz, D.; Nowacki, A.; Liberek, B. Characteristic ^{1}H NMR Spectra of β-D-Ribofuranosides and Ribonucleosides: factors driving furanose ring conformations. *RSC Adv.* **2022**, *12*, 29223–29239. doi: 10.1039/d2ra04274f
17. Tomm, H.A.; Ucciferri, L.; Ross, A.C. Advances in Microbial Culturing Conditions to Activate Silent Biosynthetic Gene Clusters for Novel Metabolite Production. *J. Ind. Microbiol. Biotechnol.* **2019**, *46*(9–10), 1381–1400. doi: 10.1007/s10295-019-02198-y
18. Muchlisyiyah, J.; Shamsudin, R.; Kadir Basha, R.; Shukri, R.; How, S.; Niranjan, K.; Onwude, D. Parboiled Rice Processing Method, Rice Quality, Health Benefits, Environment, and Future Perspectives: A Review. *Agriculture*, 13, 1390, **2023**. doi: 10.3390/agriculture13071390
19. Geris, R.; de Jesus, VET; da Silva, AF.; Malta, M. Exploring Culture Media Diversity to Produce Fungal Secondary Metabolites and Cyborg Cells. *Chem and Biod.*, **2024**. doi: 10.1002/cbdv.202302066
20. Boonphong, S.; Kittakoop, P.; Isaka, M.; Thebtaranonth, Y. et al. Multiplolides A and B, New Antifungal 10-Membered Lactones from *Xylaria multiplex*. *J. Nat. Prod.* **2001**, *64*(7). doi: 10.1021/np000291p
21. Hu, M.; Yang, X.Q.; Wan, C.P.; Wang, B.Y.; Yin, H.Y. Potential antihyperlipidemic polyketones from endophytic *Diaporthe* sp. JC-J7 in *Dendrobium nobile*. *RSC Advances*. 8, **2018**. doi: 10.1039/C8RA08822E

22. Kaur, B.; Singh, P. Epoxides: Developability as Active Pharmaceutical Ingredients and Biochemical Probes. *Bioorg. Chem.* **2022**, *125*. doi: 10.1016/j.bioorg.2022.105862
23. Aparicio, J.F.; Fouces, R.; Mendes, M.V.; Oliveira, N.; Martín, J.F. A complex Multienzyme System Encoded by Five Polyketide Synthase Genes is Involved in the Biosynthesis of the 26-membered Polyene Macrolide Pimaricin in *Streptomyces natalensis*. *Chemistry & Biology* **2000**, 7(11), 895-905. doi: 10.1016/s1074-5521(00)00038-7
24. Ikeda, H.; Òmura, S. Biosynthesis, Regulation, and Genetics of Macrolide Production. In: Macrolide Antibiotics: Chemistry, Biochemistry, and Practice. *Elsevier*, **2003**; Volume 2, pp. 285-326. doi: 10.1016/B978-0-12-526451-8.X5000-0
25. Gao, Y.Q.; Du, S.T.; Xiao, J.; Wang, D.C.; Han, W.B.; Zhang, Q.; Gao, J.M. Isolation and Characterization of Antifungal Metabolites from the Melia azedarach-Associated Fungus *Diaporthe eucalyptorum*. *J Agric Food Chem*. 68(8):2418-2425, **2020**. doi: 10.1021/acs.jafc.9b07825.
26. Zhang, Y.; Guo, S.; Xie, C.; Fang, J. Uridine Metabolism and Its Role in Glucose, Lipid, and Amino Acid Homeostasis. *Biomed Res. Int.* **2020**, 7091718. doi: 10.1155/2020/7091718
27. Karimi Khezri, M.; Turkkan, A.; Koc, C.; Salman, B.; Levent, P.; Cakir, A.; Kafa, I. M., Cansev, M.; Bekar, A. Uridine Treatment Improves Nerve Regeneration and Functional Recovery in a Rat Model of Sciatic Nerve Injury. *Turkish Neurosurgery*, **2022**, *32*(6), 935-943. doi: 10.5137/1019-5149.JTN.36142-21.2
28. Baumel, B.S.; Doraiswamy, P.M.; Sabbagh, M.; Wurtman, R. Potential Neuroregenerative and Neuroprotective Effects of Uridine/Choline-Enriched Multinutrient Dietary Intervention for Mild Cognitive Impairment: A Narrative Review. *Neurol. Ther.* **2021**, *10*(1), 43–60. doi: 10.1007/s40120-020-00227-y
29. Arbour C.A.; Imperiali B. Uridine natural products: Challenging Targets and Inspiration for Novel Small Molecule Inhibitors. *Bioorg Med Chem*. **2020**, 28(18):115661. doi: 10.1016/j.bmc.2020.115661.
30. Keller, N.P.; Turner, G.; Bennett, J.W. Fungal Secondary Metabolism—From Biochemistry to Genomics. *Nat. Rev. Microbiol.* **2005**, *3*(12), 937–947. doi: 10.1038/nrmicro1286
31. Brakhage, A.A. Regulation of Fungal Secondary Metabolism. *Nature Reviews Microbiology* **2013**, 11(1), 21-32. doi: 10.1038/nrmicro2916
32. Raaijmakers, J.M., Mazzola, M. Diversity and Natural Functions of Antibiotics Produced by Beneficial and Plant Pathogenic Bacteria. *Annual Review of Phytopathology* **2012**, 50, 403-424. doi: 10.1146/annurev-phyto-081211-172908
33. Netzker, T.; Fischer, J.; Weber, J.; Mattern, D.J.; König, C.C.; Valiante, V.; Brakhage, A.A. Microbial communication leading to the activation of silent fungal secondary metabolite gene clusters. *Frontiers in Microbiology* **2015,** 6, 299. doi: 10.3389/fmicb.2015.00299
34. Traut, T. W. Physiological concentrations of purines and pyrimidines. *Molecular and Cellular Biochemistry* **1994**, 140(1), 1-22. doi: 10.1007/BF00928361
35. Rolfes, R. J. Regulation of purine nucleotide biosynthesis: in yeast and beyond**.** *Biochemistry and Cell Biology* **2006**, 84(6), 878-886. doi:10.1139/o06-134
36. Mousa, W.K.; Raizada, M.N. Biodiversity of genes encoding anti-microbial traits within plant-associated microbes. *Frontiers in Plant Science* **2015**, 6, 231. doi:10.3389/fpls.2015.00231
37. Kusari, S.; Singh, S.; Jayabaskaran, C. Biotechnological potential of plant-associated endophytic fungi: hope versus hype. *Trends in Biotechnology* **2018**, 36(9), 898-908. doi:10.1016/j.tibtech.2018.04.006
38. Newman, D. J.; Cragg, G. M. Natural Products as Sources of New Drugs over the Nearly Four Decades from 01/1981 to 09/2019. *Journal of Natural Products* **2020**, 83(3). doi: 10.1021/acs.jnatprod.9b01285?ref=pdf
39. Bills, G.F.; Gloer, J.B. Biologically active secondary metabolites from the fungi. *Microbio Spectrum* **2016**, 4(6), 1-32. doi: 10.1128/microbiolspec.FUNK-0009-2016